RMIT UNIVERSITY

DESIGNING AN AERODYNAMICS PACKAGE FOR THE RMIT FSAE CAR

Supervisor: Simon Watkins

Second Supervisor: Sherman Chung

Student: Hashan Mendis

Student Number: s3449757

Special thanks to Robert Carrese, Nish Joseph and Riccardo Pagliarella for helping out throughout the project.

ABSTRACT

The Formula Society of Automotive Engineers (FSAE) competition allows students to design, manufacture and race formula style race cars against other teams. The objective of this study is to design an aerodynamic package to stay competitive by maximising points. Analysis of the points system and events concluded that 38 points could be gained. A decision matrix was used to determine development should focus on front and rear wings. Using a lap simulator, the coefficient of lift (Cl) of the car needed to be 1.7, the centre of pressure (COP) placed 10% forward of the centre of gravity (COG) to reduce understeer resulting in a front wing Cl of 1.5 and rear wing Cl of 1.6. Using ANSYS CFX a 2D design of experiments (DOE) was conducted to evaluate profile parameters, 3D simulations to validate DOE before implementing into chassis. The chassis was then simulated in a straight line, pitch and yaw. The results evaluated the aerodynamic package was able to make a Cl of 1.8 in a straight line with a COP 10% in front of the COG. In pitch, Cl increased by 12%, with a COP 5% in front of the COG. In yaw the Cl decreased by 26% with a COP 11% in front of the COG. The designed package was able to make the Cl required with a COP in front of the COG keeping RMIT competitive.

ABBREVIATIONS

FSAE- Formula Society of Automotive Engineers.

Computational Fluid Dynamics - CFD

Coefficient of lift - Cl

Centre of Pressure - COP

Centre of Gravity – COG

Coefficient of Drag –Cd

Design of experiments - DOE

INTRODUCTION

The Formula SAE-Australasia competition allows student engineers to design, fabricate, develop and compete with small formula style vehicles against other universities. The competition is broken up into static and dynamic events. Static events evaluate the design, cost and business plan where dynamic events tests dynamic performance, reliability, durability and fuel efficiency. The dynamic events consist of acceleration, skid pad, autocross and endurance events. The points breakdown can be found at the FSAE-A website. [2]

Aerodynamic downforce is used to increase normal force exerted by the tire, increasing cornering speed, resulting in a faster lap times. The increase in downforce comes with a drag penalty decreasing fuel efficiency, max speed and linear acceleration. The package increases vehicle mass and COG height which negatively effects dynamic performance.

RMIT's 2015 car designated R15 did not have an aerodynamics package, requiring one to be designed for the 2016 competition to stay competitive.

Objective

Design an aerodynamics package that can keep RMIT competitive by increasing points.

Methodology

Initially an analytical approach was undertaken in order to outline the constraints of the system determining overall downforce and points gain.

Simulations using ANSYS was used to understand the flow structure and how it changed in pitch, roll and yaw.

ANALYTICAL APPROACH

There are multiple variables that need to be taken into account when designing an aerodynamic package. The events analysed to understand where aerodynamics improve lap time, Optimum Lap used to determine overall Cl of the car and decision matrix created to allocate resources. By evaluating COP location, front and rear wing Cl was determined, front wing ground clearance evaluated and drag analysed.

Dynamic Event Analysis

Each event evaluates different aspects of the dynamic performance of the car. The acceleration event evaluates the car's acceleration in a 75m straight line. Skid pad measures the car's cornering ability, layout of the track consists of a pairs of concentric circles 18.25 m apart in a figure of eight pattern. Autocross evaluates the car's manoeuvrability on a 0.8 km tight course. Endurance evaluates overall performance, durability and reliability totalling 22km. Efficiency measures the tuning performance, evaluated by measuring the energy consumed and endurance lap time. [1]

Analysis was conducted by the team to determine the relationship between skid pad, acceleration and autocross events. Reliability is a dominating factor in endurance, assuming a reliable car, competitive times in autocross translated to success in endurance. The results from the previous years was graphed in Appendix A, showing a strong correlation between success in skid pad against autocross indicating importance of lateral over linear acceleration. [2-6]

Target Downforce using Optimum Lap

Optimum Lap is a point mass, quasi-steady state simulator. It is a simplistic model of the car able to capture global trends. Even through the point mass simulator doesn't account for weight transfer or transient effects the results correlate within 10% of logged data.[7]

Skid pad was used to determine how much downforce is required to win because it evaluates the car's cornering ability, the track is easily replicated, consistent between years with known points designation. With calibration, the test can be used in future to develop the aerodynamic package.[1, 8, 9]

An Optimum Lap model of the winning 2015 car was created using the information available, (assuming Cl was taken in a straight line) engine and transmission data used from R15. The model was calibrated until lap times correlated with track times by 1%. The R16 concept was an iteration of R15 as outlined in Appendix B, adding 10kg representing aerodynamics package, then increasing Cl to 1.4 to obtain a winning skid pad time. The acceleration and autocross track was added into the program to estimate points gained.

Comparing R15 and R16, points analysis outlined in Appendix C, showing 38 points gain using an aerodynamics package. Due to the added drag, acceleration decreases 4.4 points, downforce increased skid pad points by 14.6, autocross increased 7 points and endurance 21 points. Fuel efficiency was not calculated as not enough information is available.

As the project aims to maximise points the Cl of the car was increased by 20% to emulate competitors improving their package resulting in a car Cl of 1.7. As mentioned Optimum Lap doesn't take into account efficiency in yaw, assuming a Cl of 1.7 can be achieved in a straight line, the 38 points can be gained.

Cornering Performance

A speed map of the 2015 autocross track with R16 concept is shown in Appendix C and used to understand the types of corners and relative speeds. The speed map shows that the cornering speeds range from 20km/h to 60km/h.

In order to determined where aerodynamics could be effective, the cornering stages - braking into a corner, mid corner, exit corner and speed range – low to high were analysed. The analysis found that at low speeds the aerodynamic forces did not dominate relying on mechanical grip. At medium to high speeds, braking into a corner the aerodynamics should aim to maximise drag in pitch in order to reduce braking distance. Mid-corner requires traction and in roll. The aerodynamics should produce the most amount of downforce. Exiting a corner low drag allows the car to accelerate out of a corner. The three cornering situations will be analysed in simulations to understand the Cl and COP.

With known vehicle parameters, difference in cornering times of R15 and R16 determined at different cornering radius in Appendix F. The analysis found that an 11 m radius - smallest autocross corner - 0.05 seconds was gained, in a 22 m radius corner 0.14 seconds was gained. The time difference between the cars are small but taking into account there are 30 corners in total, a 0.05 gain in every corner returns a 1.5 second gain in autocross and 35 seconds gain in endurance. This doesn't take into account the time lost accelerating due to aerodynamic drag however it shows that a small gain in a corner can add up over track.

Decision Matrix

The decision matrix in Appendix D was used to determine where resources should be allocated. The devices chosen to evaluate were front and rear wing, side pods and diffuser against factors outlined. A multiplier was assigned to each factor depending on its importance - low number having high significance - with on track validation ranking highest.

The matrix outlined device hierarchy front wing, side pods, rear wing then diffuser. Side pod were designed from the previous year with re-usable moulds and the downforce required would be generated by front and rear wings. The diffuser was considered from the current package but it was determined that time needed to integrate and simulate wouldn't be possible.

Analysing Centre of Pressure

When designing an aerodynamic package the COP allows the car to act in a predictable manner.[5]The COP is where the net moment created by all aerodynamic forces is equal to zero and can also be used to tune the handling capability of the car.[3](Appendix G) In order to reduce understeer present in R15 the aerodynamic bias is set forward of the COG.

The COP will start to migrate when the force exerted by the aerodynamics devices change which occurs during breaking, roll and yaw. It is important to keep the COP either side of the COG, failure to do so will reduce the handling capability of the car.

No information was found on the COP migration being sensitive to suspension setup and the sensitivity of the aerodynamics devices. An assumption was made that the COP would migrate 10% which could be track tested and refined. The COP of a double element wing is 40% of the chord and 60% of the chord for triple element.[2, 3] The COG of the system is 56% from the front of the car.

As the COG is known, COP migration assumed, COP of the wings and relative positions, Cl of the wings can be determined. The moment around the COP was resolved. The front wing requires a Cl of 1.56 ($A = 0.806m^2$) and the rear wing a Cl of 1.67($A = 0.63m^2$). The Cl of the chassis and side pod was neglected as their contribution was small.[10-12]

Front Wing Ground Clearance

Ground clearance of the front wing is important to determine to ensure it isn't damaged. As the front wing is sensitive to ground clearance it will affect the COP of the car and overall downforce.

To determine the minimum ground clearance, Optimum K was used to determine weight transfer in braking and roll. Optimum K simulates suspension geometry under load. [7] Using data from Optimum K, under 1.6 G's of braking the car experience 1.2° of pitch, a corner at 1.6 G's equated to 1.5° of roll. Taking into account 10 mm of wing deflection minimum ground clearance is 40mm. Under these conditions the front wing shouldn't bottom out.

Drag Analysis

Drag needs to be analysed in order to understand how it affects max speed.

At a critical speed, power created by the engine is required to overcome the drag force. By using a Cd of 1.0, similar to the 2012 Monash, critical speed was determined to be 150km/hr. Track speed is limited to

110km/hr by rules inferring drag won't limit top speed.[13]

It is important to take into account the engine efficiency is primarily dictated by the tuning set up where most of the points can be gained compared to low drag wings.

SIMULATIONS

The aerodynamics package requires an overall Cl of 1.7, front wing Cl of 1.5, rear wing Cl of 1.6, a COP 10% in front of the COG and a max Cd of 1.0.

In order to maximise downforce, the front wing was placed as far forward as possible and extended from hub to hub resulting in a 620 mm chord length. Due to the flow disturbance of the drive, the rear wing was placed 250 mm behind the rear wheel, underneath 1200 mm from the ground and above the helmet, to reduce the effect of the helmet wake. The rear wing had a chord length of 700 mm.[1]

CFD Design Methodology

When designing the wings, the flap angle, flap chord length, gap, overlap and gurney sizes needed to be evaluated.

The extra flaps create more downforce by increasing the effective camber, angle of attack and the interaction between the main element and flaps. The gap between elements allow air from the upper surface to bleed into the lower surface, the converging slot increases velocity, causing a pressure drop. The increased velocity adds energy to the boundary layer helping delay flow separation. The slots also ensure the wake of the main element doesn't affect the formation of the flap boundary layer. The gurney flap attached to the trailing edge, creating a high pressure region and counter rotating vortices; the suction creates a drop in pressure increasing downforce. These factors combined increase the pressure difference between the upper and lower surfaces increasing downforce. [2, 3]

The rear wing was analysed first because it had one less variables and the parameters would be used to analyse the front wing.

The front wing used Clarke-Y-s1223 double element and rear wing triple s1223. [14]

A design of experiments was conducted in 2D to maximise downforce, the chord wise flow results in an even pressure distribution overstating coefficients. It doesn't take into account vorticity and different pressure regions interacting however using a constant set up general trends can be deduced with simulations taking minutes.

A partial design of experiments was then conducted in 3D focusing on areas that would yield high downforce. In 3D, due to vortices and different pressure fields interacting, the air flow travels chord and span wise. The change in flow, changes the pressure distribution and hence pressure coefficients. 3D simulations can take hours to solve but accurately predict flow fields of complex geometry. To reduce computational time, the front and rear wings were optimised in isolation and fitted onto the car to re-test.

Rear Wing

2D CFD Rear Wing

Before the 2D design of experiments was conducted a domain and mesh study was conducted to ensure independence.

The domain study ensured the domain didn't affect the pressure distribution of the wing by placing the walls at an acceptable distance and the outlet placed after the wake. The overall wing chord was used to create a dimensionless domain, which allowed the results to be used in following simulations. Table 1 outlines the results of the domain study where L = 700 mm.

Parameter	Length
Outer Upwind	5L
Outer Downwind	15L
Outer Upper	5L
Inner Upwind	0.5L
Inner Downwind	2L
Inner Upper	1L
Domain Thickness	1 mm

Table 1-Domain study

A mesh study was then performed to ensure independence. It consists of tetrahedron elements that are able to contour to the complex geometry, an inner volume sizing, edge sizing around the wing, an inflation layer and swept elements. The mesh was refined until Cl and Cd were constant resulting in meshing parameters outlined in Table 2.

Parameter	Size (mm)
Inner Domain Volume Sizing	100
Edge Sizing	5
Wing Y+	1

Table 2- Mesh Study

While running the simulations the model set up parameters are outlined in Table 3.

Parameters	Value
Inlet	40 km/hr
Wall	Free Slip Wall
Ground	40 km/hr No Slip Wall
Outlet	0 Relative Pressure
Turbulence Model	k-w SST

Table 3-Set Up

A k-w SST turbulence model accurately model the boundary layer requiring a Y+ of 1. [15]

With a domain and mesh study established the parameters were tested.

Initially the element chord lengths were altered against flap angles with the results in Appendix H. Graphed is the data from 30% and 40% chord length of the two flap elements against flap angles. The main element was set to an AOA of 0, flap 1 indicated in legend and flap 2 on the axis. The angles were taken from horizontal. The results showed a unimodal graph, downforce increases until the adverse pressure gradient was unable to be overcome, separation insured, decreasing downforce. This showed that the optimum flap chord length is 40%, flap 1 at 30 degree and flap 2 between 40 to 50.

Using the flap chord length, the remaining parameters were tested by changing one variable against another. The study showed the parameters below in Table 4 needed to be tested in 3D.

Parameters	Dimension
Flap Chord	40 %
Gap	1 %
Overlap	4 %
Gurney	4 %
Main AOA	0°
Flap 1 AOA	30°
Flap 2 AOA	45°

Table 4-Dimensions from 2D rear wing study

3D CFD Rear Wing

As discussed after the 2D design of experiments a 3D partial design of experiment was conducted to focus on areas of high downforce. The domain from before and mesh study was conducted in 3D with the results in the Table 5. Figure 1 shows the mesh on the symmetry plane of the inner domain and swept elements.

Parameter	Size (mm)
Inner Domain Volume Sizing	100
Face Sizing on rear wing	10
Wing Y+	11
Swept Elements	Bias applied

Table 5- Mesh study of 3D rear wing

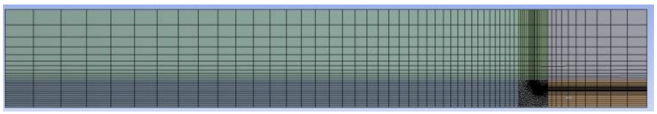

Figure 1-Mesh on symmetry plane

The mesh study as seen in Appendix I, found that a Y+ of 11 was acceptable for the flow condition. This reduced inflation elements, reducing computation time while accurately predicting the flow structure.

Using the 2D experiment the parameters in 3D were tested. The flap angles in Table 4 were used as a starting point. The flaps were increased until separation, gap and overlap was then tested. Table 6 outlines the parameters determined from the 3D design of experiments.

Parameters	Dimension
Flap Chord	40%
Gap	1%
Overlap	4%
Gurney	4%
Main AOA	0°
Flap 1 AOA	40°
Flap 2 AOA	60°

Table 6-Optimum Rear Wing parameters from the 3D DOE

CFD as seen in Figure 2 shows a stagnation region at the leading edge of the main element as expected. Velocity increases at the lower surface causing low pressure, the air for the top main surface is bled into the lower flap surface of the flap with the converging gap increasing speed, causing a pressure drop. There was slight separation of the second flap.

In free stream the parameters gave a Cl of 2.6 and Cd of 1.0. When the rear wing is added to the car, due to the recirculation region created by the driver it is expected to decrease Cl by 40% and increase Cd. [13] This should give the downforce required.

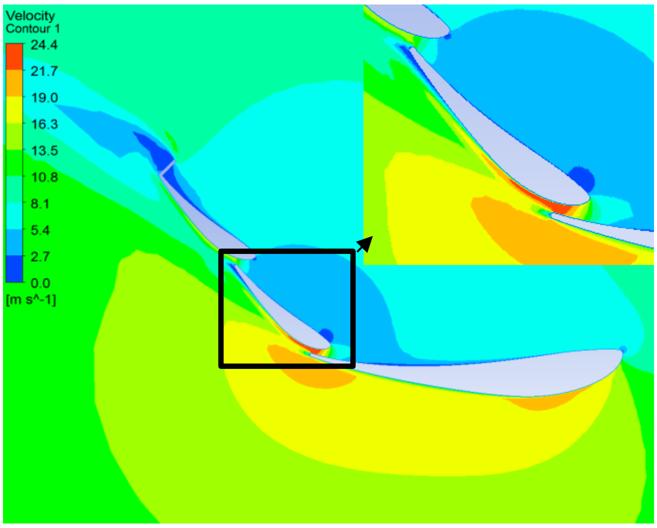

Figure 2-Velocity on the symmetry plane

End plate length was changed, in order to nondimensionalise the analysis, the length of the end plate was divided by the thickness of the main element. Appendix J, outlines the data. It shows that as the length increased, downforce increased and drag decreased. The end plates create a clockwise vortex at the top edge, and counter clockwise vortex at the bottom edge. The vortex changes the flow, which changes the pressure distribution. By increasing the end plate length, the bottom vortex is moved further away from the bottom surface, reducing its effect, however a larger end plate increases rotational inertia decreasing yaw rate. The end plate length was kept to 3 times the thickness as it was able to make the downforce required with its effect on yaw requiring track testing.

In yaw the end plates block air flow causing separation, a section was taken out according to the pressure distribution on the end plate as shown in Figure 3 by the black dotted line.

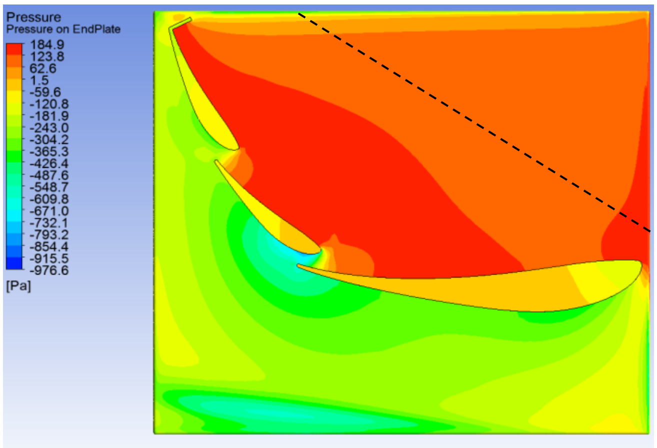

Figure 3-Pressure on end plate

Front Wing

2D CFD Front Wing

Using the parameters for the rear wing a 2D design of experiment was conducted.

The design of experiments showed that when the flap angle increased, the pressure gradient would increases causing separation. This effect was exaggerated with the wing was in ground clearance. Due to mass continuity, as the area between the element and ground decrease, velocity increases causing a large pressure drop.

The ground clearance study was analysed to show maximum downforce at 70 mm ground clearance, by doing so would increase the complexity of the design and lengthen the manufacturing process, hence the front wing was kept at 50 mm. (Appendix K) The study also showed the front wing was as sensitive to ground clearance showing an overall change in Cl by 8%. The results of the 2D study are outlined in Table 7.

Parameters	Dimension
Flap Chord	30 %
Gap	1 %
Overlap	4 %
Gurney	4 %
Main AOA	0°
Flap 1 AOA	20°
Ground Clearance	50 mm

Table 7-Optimum Front Wing Parameters from 2D DOE

3D CFD Front Wing

Using the mesh and domain stated in Table 1 and 5, the 2D front wing DOE was validated in 3D, results outlined in Table 8.

Parameters	Dimension
Flap Chord	30 %
Gap	1 %
Overlap	4 %
Gurney	4 %
Main AOA	0°
Flap 1 AOA	30°
Ground Clearance	50 mm

Table 8-Optimum Front Wing Parameters from 3D DOE

The 3D analysis showed a large vortex being created on the bottom edge of the front end plate due to the low pressure region under the wing as seen in figure 4. The vortex had a large effect on the pressure distribution of the main element reducing downforce. As discussed, the vortex interferes with the pressure distribution reducing efficiency.

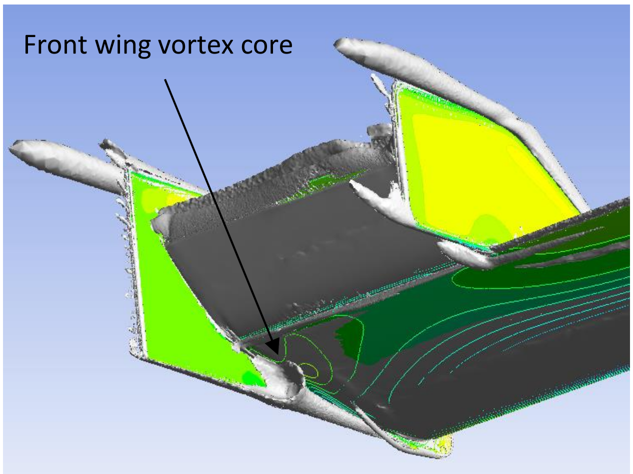

Figure 4-Vortex on Front Wing

As before sections were taken out according to the pressure distribution. A 19 mm foot and side plates were added to the end plate, it decreased the intensity of the vortex at the bottom and moved the top vortex away from the wing. The pressure distribution of the wing improved increasing Cl by 9%, resulting in a Cl of 2.0 and Cd of 0.4.

Full Car Simulation

As a wind tunnel experiment was conducted on the chassis and the set up and mesh parameters were compared. The radiator was excluded from the simulation due to complexity.

Wind Tunnel Model

The CAD was created using Solidworks and is shown in Figure 5, the wind tunnel model is seen in Figure 6.

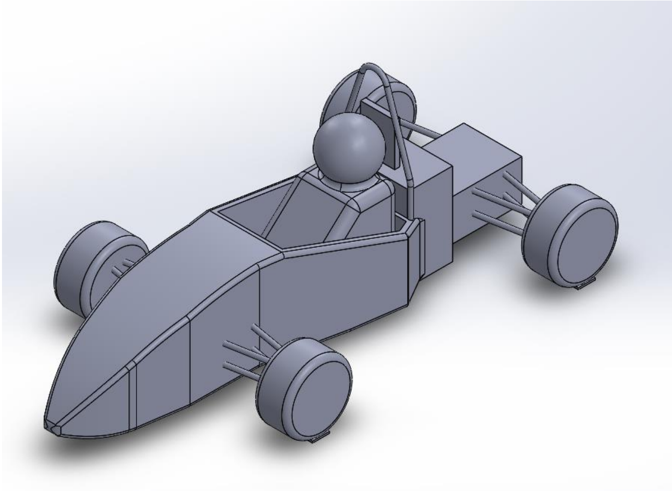

Figure 5-CFD CAD Model

Figure 6-Printed model in the wind tunnel

The car model was simplified; an open cock pit was used around the dummy driver, the engine and transaxle was replaced with two cubes, due to the geometry the flow will separate, adding detailed components would increasing meshing and computational time with little effect on results. The results of the mesh study and set up are shown below in Table 9.

Mesh	
Relevance Centre	Coarse
Inner Domain Volume Sizing	200 mm
Chassis + Side Pod Y +	30
Wheels Y +	11
Set Up	
Parameters	Value
Inlet	40 km/hr
Wall	Free Slip Wall

Ground	40 km/hr No Slip Wall
Outlet	0 Relative Pressure
Symmetry Plane	Symmetry
Chassis	No-slip Wall
Wheels	Free Slip Wall
Turbulence Model	k-w SST

Table 9-Results of the mesh and set up

The comparison of the wind tunnel and CFD results are shown in Table 10 with a reference area of $0.7m^2$. As pressure gradients don't dictate separation a Y + of 30 was used after performing the mesh study, -Cl indicating lift.

	Cl	Cd
Wind Tunnel	-0.19	0.57
CFD	-0.22	0.55
% Difference	15%	4%

Table 10-Comparision between wind tunnel and CFD

Lift shows a large deviation from the wind tunnel model due to the boundary layer, effecting pressure distribution of the under body. Not enough information was present to model the boundary layer. Drag of the CFD model is within 4% of the wind tunnel model which is an acceptable level. [10, 16]

These results emphasis that without accurate CFD-wind tunnel validation the final results are within an error margin. This is another reason why in this application CFD is used as a parametric study to capture general trends and then validate on track.

The model was then adjusted, adding the side pods, taking away suspension arms and adding rotating wheels as seen in Figure 7.

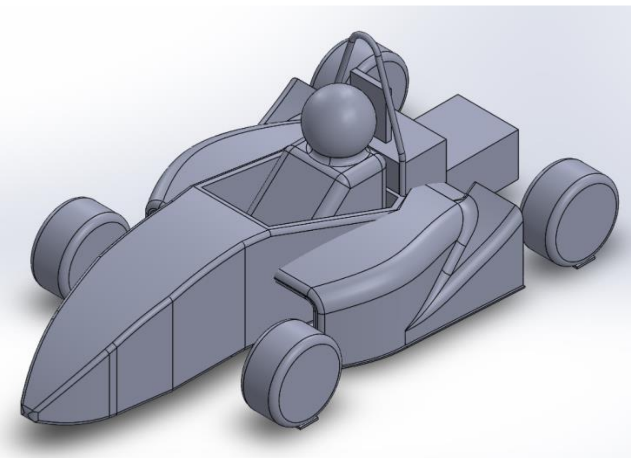

Figure 7- CAD model with Side Pods

The difference between the two models seen in Table 11.

	Cl	Cd
Model without Side pods	-0.22	0.55
Model with Side pods	-0.10	0.60
% Difference	54%	9%

Table 11- Comparison between two models

The rotating wheels and side pods add 9% in drag and the side pods reduced lift by 54%.

The flow shows stagnation at the nose as seen in Figure 8, air flow is then diverted above and below the car. The upper surface separates at the open cockpit due to the sharp geometry change. The open cockpit experiences a large recirculation region increasing drag. Flow stagnates around the helmet separating at

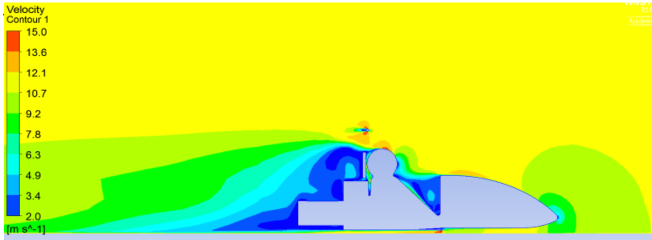

Figure 8-Velocity on symmetry of chassis

Aerodynamic Package – Straight Line

With parameters and positions of the wings known, the wings were added to the car as shown in Figure 9. The rear wing mounting rods were added as they effect the lower surface of the rear wing.

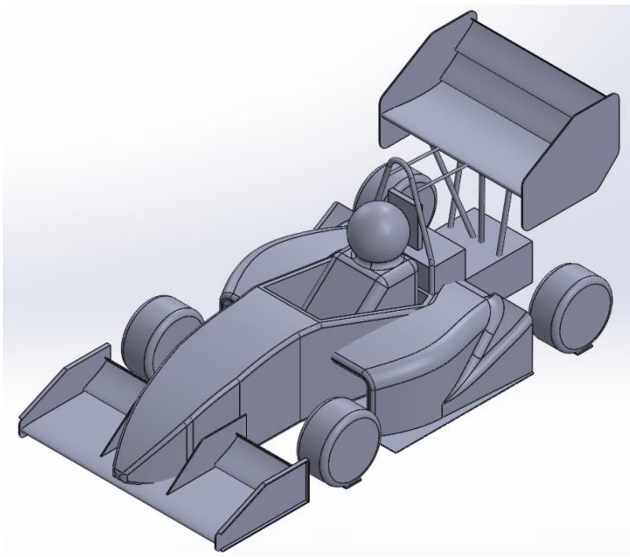

Figure 9-CAD with Aerodynamic Package

The results of the mesh study and set up is shown in Table 12. Figure 10 shows the mesh on the symmetry plane displaying swept elements. Figure 11 shows the surface mesh on the chassis and wings.

Mesh	
Relevance Centre	Coarse
Inner Domain Volume Sizing	100 mm
Wing Profile Y+	11
Chassis, side pod, end plates Y+	30
Face Sizing on profile	10 mm
Ground	5 inflation layers
Set Up	
Parameters	Value
Inlet	40 km/hr
Wall	Free Slip Wall
Ground	40 hm/hr No Slip Wall
Outlet	0 Relative Pressure
Symmetry Plane	Symmetry
Chassis, wings	No-slip Wall
Wheels	55 rad/s No Slip Wall
Turbulence Model	k-w SST

Table 12- Mesh and Set up of Chassis with Aero Package

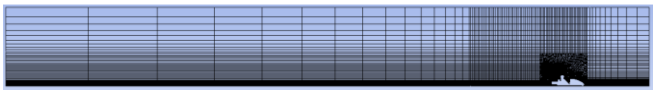

Figure 10- Mesh on symmetry plane

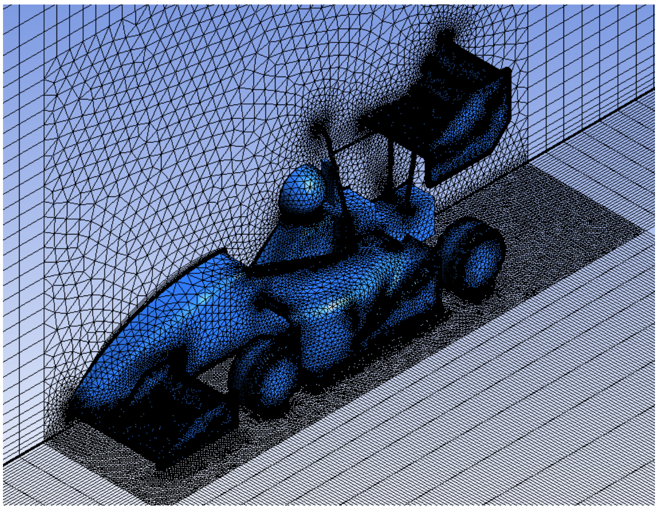

Figure 11- Surface mesh of chassis

The results are summarised in Table 13 below. The reference area for the front wing is $0.806\ m^2$, rear wing $0.63\ m^2$, chassis $0.7\ m^2$, overall $1.3\ m^2$.

Component	Coefficient
Front Wing Cl	1.65
Front Wing Cd	0.28
Rear Wing Cl	1.90
Rear Wing Cd	0.66
Chassis Cl	-0.16
Chassis Cd	0.64
Overall Cl	1.86
Overall Cd	0.84
COP Bias	47%

Table 13- Results of Straight Line CFD

Initially the rear wing was making too much downforce so the rear flap element was set to 40°.

It is evident from testing in isolation to with the car how the flow fields change. The effect of the front wing washed the air up towards the rear wing. The front end plate vortices can also be seen to travel down the car. The end plate vortex travels around the tire and the bottom vortex is angled towards the side pod and down the floor. It can also be seen that due to the front wing wake, the air entering the side pods is of lower velocity which will effect cooling. The rotating wheels make the air turbulent in front of front wing, causing separation, reducing efficiency.

Due to the drivers helmet, engine and roll hoops the air interacting with the rear wing is turbulent reducing the efficiency.

The mounting system has a direct effect on the pressure distribution. The rods create a small wake decreasing efficiency. The mounting system was kept in the middle as the air was turbulent due to the helmet.

The results show a 20% reduction in Cl of the front wing and 37% in the rear wing compared to isolation. The COP bias is 1% forward from the intended analysis which is acceptable.

Aerodynamic Package – Pitch

The car was placed in at 1.5° in pitch representing the car in full dive under breaking. Total down force increased by 12% with a COP of 51%, 5% in front the COG.

Separation of the main element of the front wing is responsible for the movement in COP as seen in Figure 12. The increase in downforce comes from the raked chassis

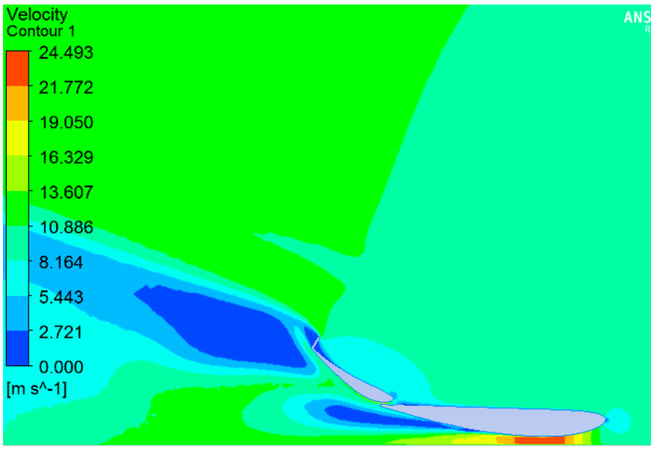

Figure 12-Velocity on front wing

Aerodynamic Package – Rotating Domain

Figure 13 shows the car in the rotating domain. The chassis was at 10° yaw, 1.5° roll and wheels at 12°. The domain was set to skid pad radius of 8.25 m, the mesh used outlined in Table 12 with a rotating reference frame. An upwind advection scheme and stationary wheels was used due time constraints.

The model set up is shown below in Table 14.

Set Up	
Domain Motion	1.375 rad/s
Domain Interface	Rotational Periodicity between inlet and outlet
Wall	Free Slip Wall
Ground	40 hm/hr No Slip Wall
Chassis, wings, wheels	No-slip Wall
Turbulence Model	k-w SST

Table 14-Set up of rotating domain

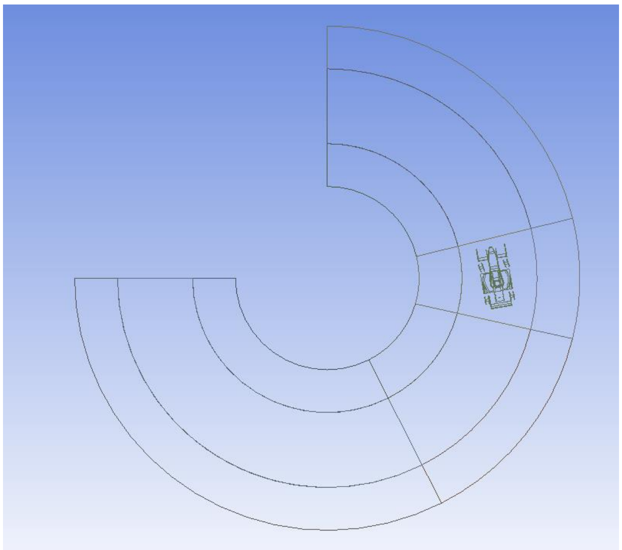

Figure 13- Rotating Domain

Due to the rotating frame the flow structure changed. As the front wing is in roll the outer portion has a lower pressure because it is closer to the ground as seen in Figure 13. There are vorticies created from the end plates but there is no separation.

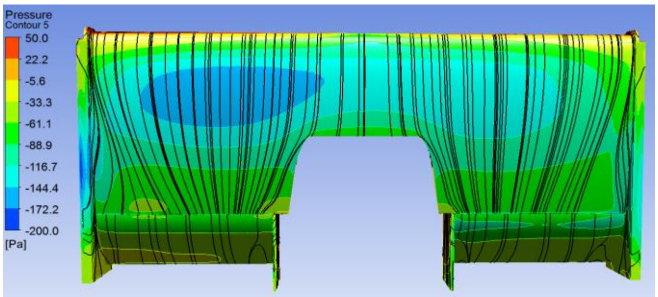

Figure 14- Pressure Distribution and streamlines on front wing

The air then separates from the front wheel creating a large vortex traveling down the side of the car. The front wing end plate creates a vortex at its top edge that seals the air flow down the car. The pressure distribution along the bottom of the rear wing shows separation at the mounting arms creating its own wake as seen in Figure 15. There isn't any separation on the lower surface however the outer side has a lower pressure distribution than the inner due to the end plate.

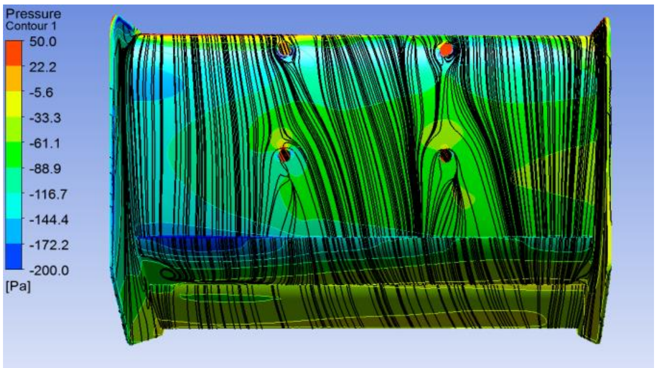

Figure 15- Pressure Distribution and Streamlines on rear wing

Due to the rotating flow the wake structure is different; the rear wing end plate and front wheel creates a large low pressure region due to separation.

The results showed a 26% drop in downforce from the straight line case with a 47% COP. The decrease in downforce is concerning however the fact that the COP is at the desired location is important. The results show the Cl of the front wing decrease by 27% and rear wing by 29%. [13]

Validation

Due to time constraints the package was not manufactured in time and tested in a wind tunnel. The CFD of the wings needs to be validated but based on the existed data variation of 8% can be expected.

CONCLUSION

In order for the RMIT FSAE car to stay competitive an aerodynamics package was designed which should be able to capture 38 points. Using Optimum Lap the Cl required to win the skid pad is 1.7, a decision matrix showed resources should be spend around the front and rear wing. The COP was set 10% in front of the COG in order to reduce understeer.

Wing profiles were tested in 2D and 3D CFD. The wings were then added to the car and simulated in a straight line, 1.5° of pitch and 10° of yaw.

The straight line resulted in a Cl of 1.8 with a COP 11% in front of the COG. In 1.5° of pitch Cl increased by 12% with a COP 5% in front of the COG. The shift in COP is attributed to separation of the front main element. The car was then placed in a rotating reference frame simulating skid pad. The package reduced Cl by 26%, however the wings lost downforce at an equal rate resulting in a COP 11% in front of the COG.

During all situations the COP is kept in front of the COG with maximum movement of 5% in pitch.

Due to time constraints wind tunnel tests weren't performed, however previous testing shows an 8% error margin.

The analysis shows that the designed aerodynamics package will have the downforce required to win skid pad and gain 38 points.

Recommendation

The followings are recommendations for the future improvement

- Validate the CFD using wind tunnel and on road testing
- In order to reduce COP movement increase the ground clearance of the front wing
- Design a triple element front wing and diffuser to increases downforce while keeping a COP in front of the COG
- Simulate different cornering radius and conditions of the FSAE track

References

[1] FSAE-A, "2015 Formula SAE Rules," 2015.
[2] S. MacBeath, *Competition Car Aerodynamics* 2015.
[3] J. Katz, *Race Car Aerodynamics*, 2015.
[4] C. Smith, *Tune to Win*, 1978.
[5] J. S. Scott Wordley "Aerodynamics for Formula SAE: Initial design and performance prediction," *SAE,* 2006.
[6] A. M. D.Bolitho, "Benchmark Analysis," 2016.
[7] O. Lap. *Optimum Lap*. Available: http://www.optimumg.com/software/optimumlap/
[8] FSAE-A. (2015). *2015 Results*. Available: http://www.saea.com.au/resources/Documents/results.pdf
[9] W. S. Murray, "Vehicle Dynamic Validation and Analysis from Suspension Forces," *Oregon State University,* 2012.
[10] G. Thomas, "FSAE Race Car Aerodynamics," *RMIT* 2012.
[11] J. Kopf, "Optimization of Aerodynamical Aspects of a FSAE Race Car," *RMIT* 2011.
[12] Ponnappa Bheemaiah Meederira, "Aerodynamic development of a IUPUI Formula SAE specification car with Computational Fluid Dynamics(CFD) analysis," *Purdue School of Engineering and Technology Indianapolis,* 2015.
[13] J. S. Scott Wordley "Aerodynamics for Formula SAE: A Numerical, Wind Tunnel and On-Track Study," *SAE,* 2006.
[14] J. G. Michael Selig, Andy Broeren, Philippe Giguere, *Summary of Low Speed Airfoil Data*, 1995.
[15] G. H. Y. Jiyuan Tu, Chaoqun Liu *Computational Fluid Dynamics: A Practical Approach*, 2007.
[16] W. Q. Benedict, "Research on rapid prototyped models for use in Automotive wind tunnel testing," 2015.

Appendix A: Competition Results

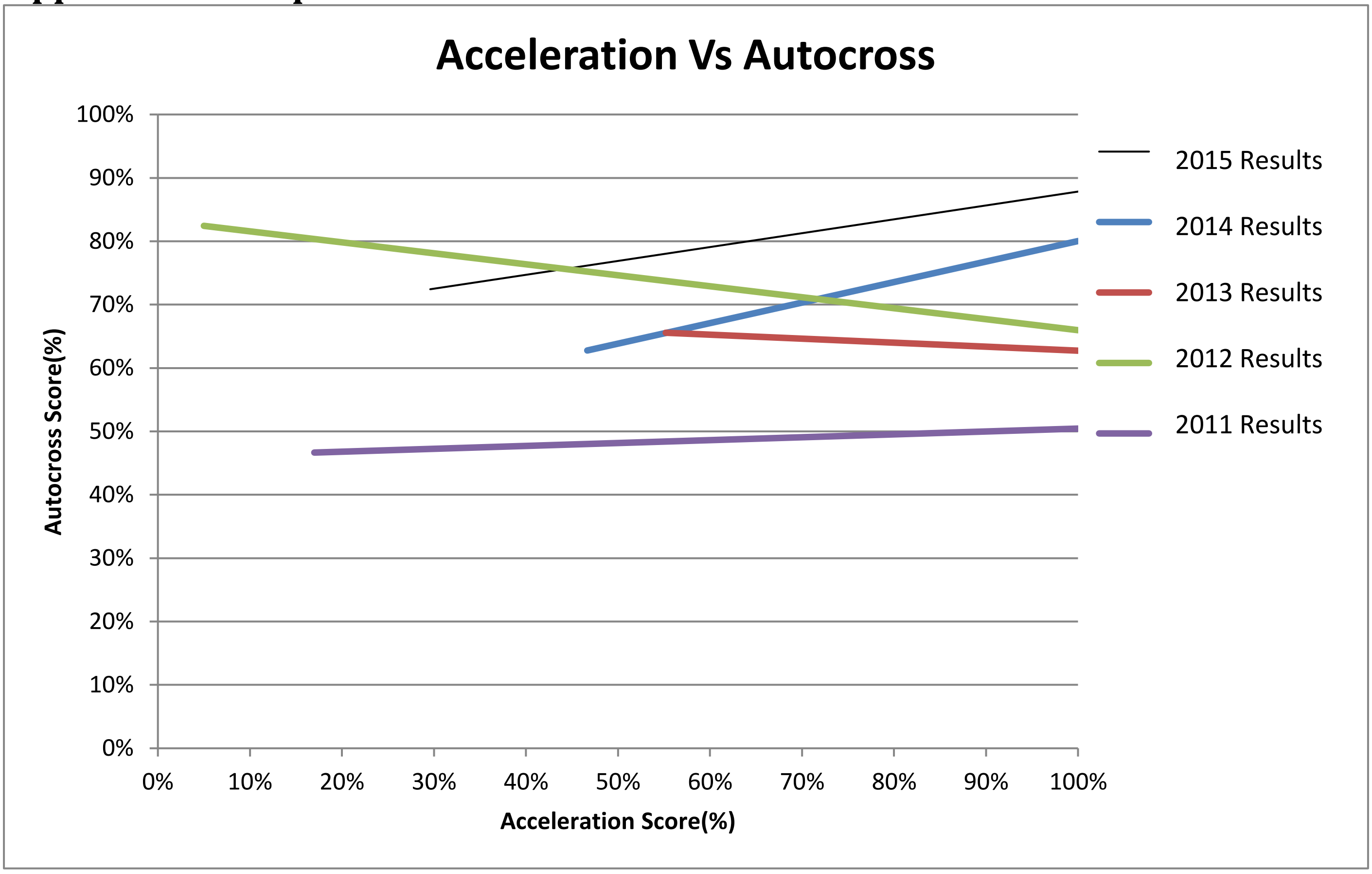

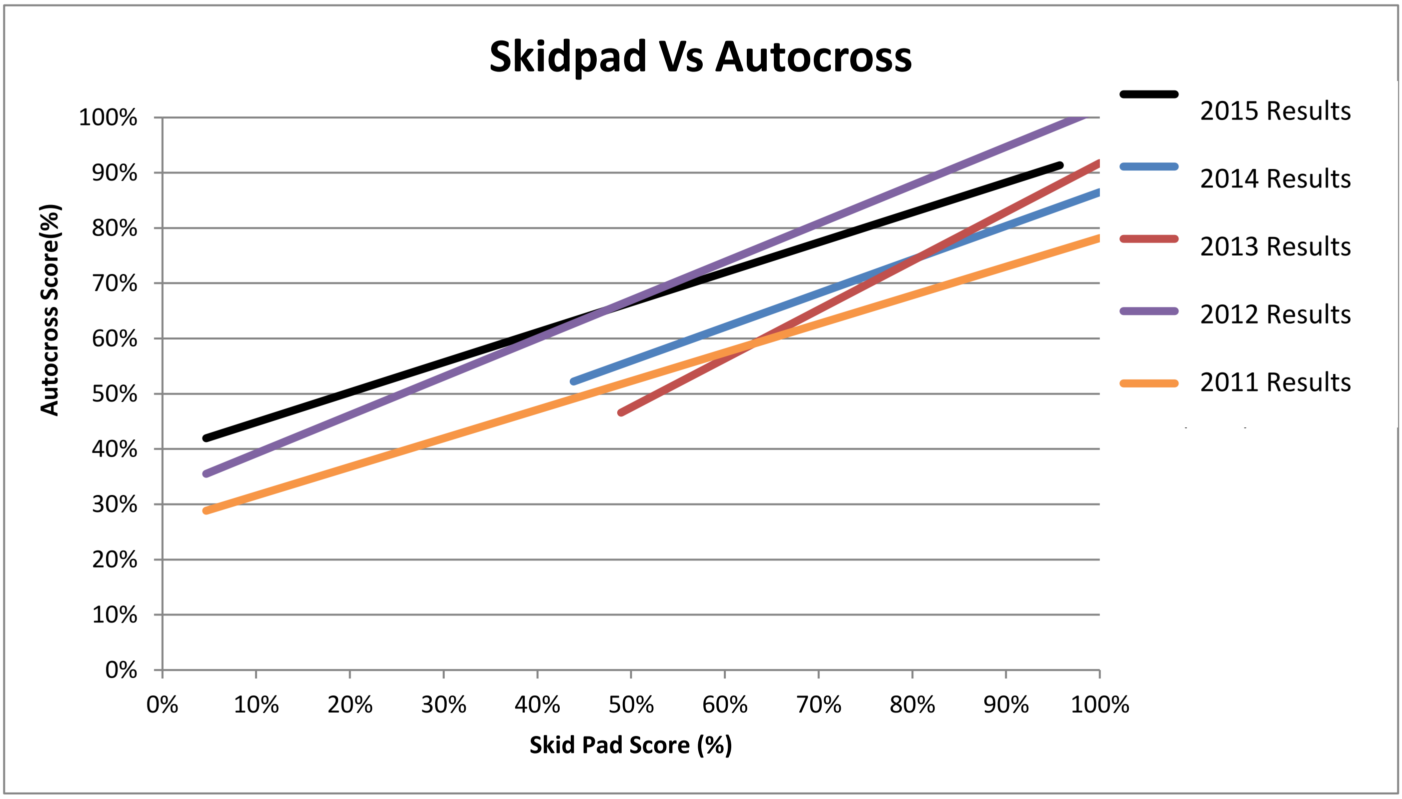

Appendix B : Optimum Lap Data

R16 Concept Data

Parameter	Value
Mass with 60kg driver(kg)	260
Frontal Area assumed(m^2)	1.3
Air Density (kg/m^3)	1.225
Cd	1.0
Cl	1.4
Tire Radius (m)	0.205
Rolling Resistance	0.03
Longitudinal Friction	1.4
Lateral Friction	1.4
Thermal Efficiency	30%
Fuel	E85
Final Drive Ratio	2.273
Drive Efficiency	90%
Engine Speed (RPM)	Engine Torque (N.m)
4800	22.40
5300	29.00
5800	31.60
6300	35.60
6800	43.50
7300	42.20
7800	46.10
8300	44.50
8800	42.20
9300	40.20
9800	46.20
10300	48.50
10800	46.80
11300	43.50
11800	42.20
Gear	Gear Ratio
1	4.5000
2	2.8000
3	1.4006
4	1.0438

Canterbury Concept Data

Parameter	Value
Mass with 60kg driver(kg)	264
Frontal Area assumed(m^2)	1.3
Air Density (kg/m^3)	1.225
Cd	1.0
Cl	1.3
Tire Radius (m)	0.230
Rolling Resistance	0.03
Longitudinal Friction	1.4
Lateral Friction	1.4
Thermal Efficiency	30%
Fuel	E85
Final Drive Ratio	2.273
Drive Efficiency	90%
Engine Speed (RPM)	Engine Torque (N.m)
4800	22.40
5300	29.00
5800	31.60
6300	35.60
6800	43.50
7300	42.20
7800	46.10
8300	44.50
8800	42.20
9300	40.20
9800	46.20
10300	48.50
10800	46.80
11300	43.50
11800	42.20
Gear	Gear Ratio
1	4.5000
2	2.8000
3	1.4006
4	1.0438

Appendix C: Points Analysis

Event	Points	R15 – No Aero	R16-Aero	Points Difference
Acceleration	75.0	68.1	63.7	-4.4
Skid Pad	75.0	59.6	74.2	14.6
Autocross	100.0	87.6	94.9	7.3
Endurance	325.0	289.0	310.2	21.3
				38.8

Appendix D: Decision Matrix

		Devices			
Factors taken into account	Multiplier	Front Wing	Rear Wing	Diffuser	Side Pod
Time needed to understand the device	2	1	2	4	3
Time taken to Design and integration	3	2	3	4	1
Time needed to Simulation	4	1	2	4	3
Resources to manufacture	5	2	3	4	1
Validation on track	1	2	2	2	1
	Total Score	24	38	58	27

Appendix E: Autocross Speed Map of R16

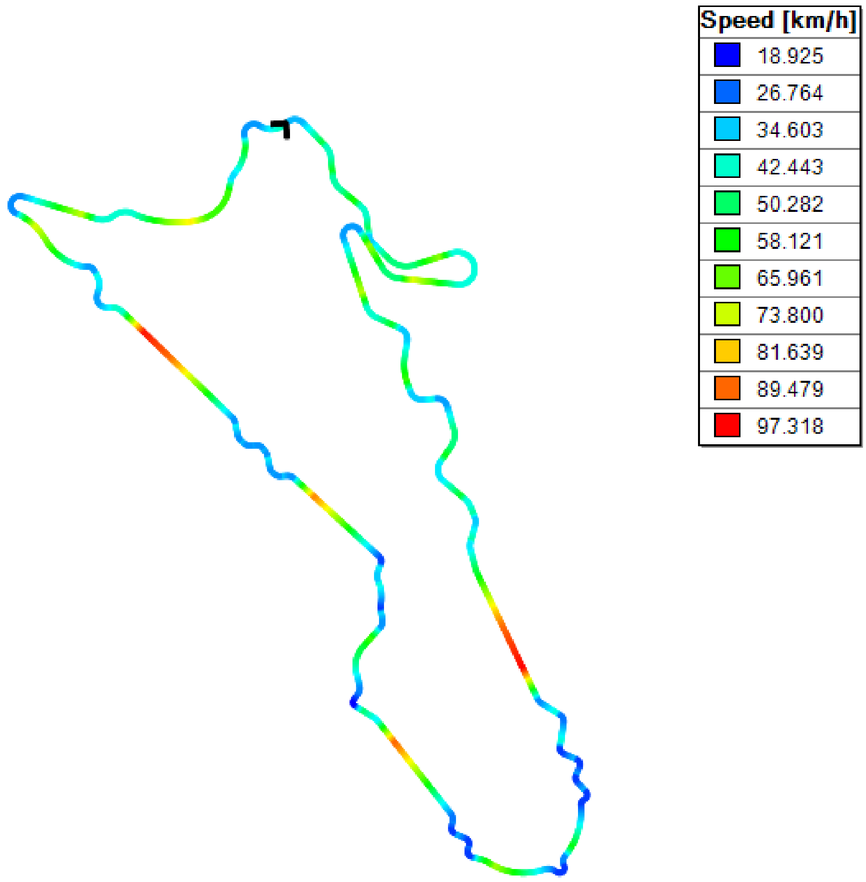

Appendix F: Cornering Analysis

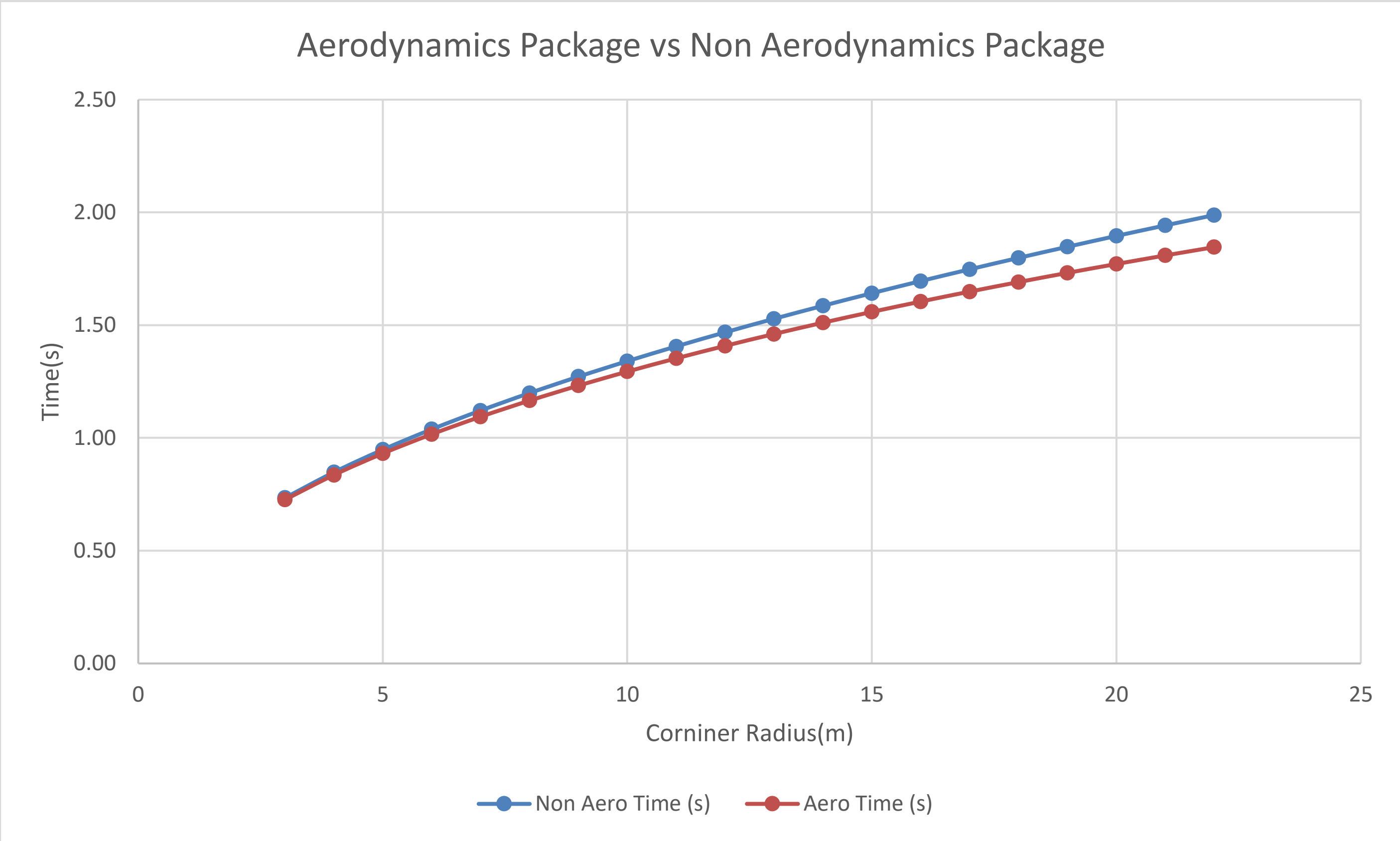

Appendix G: Determining Cl of Front and Rear Wing

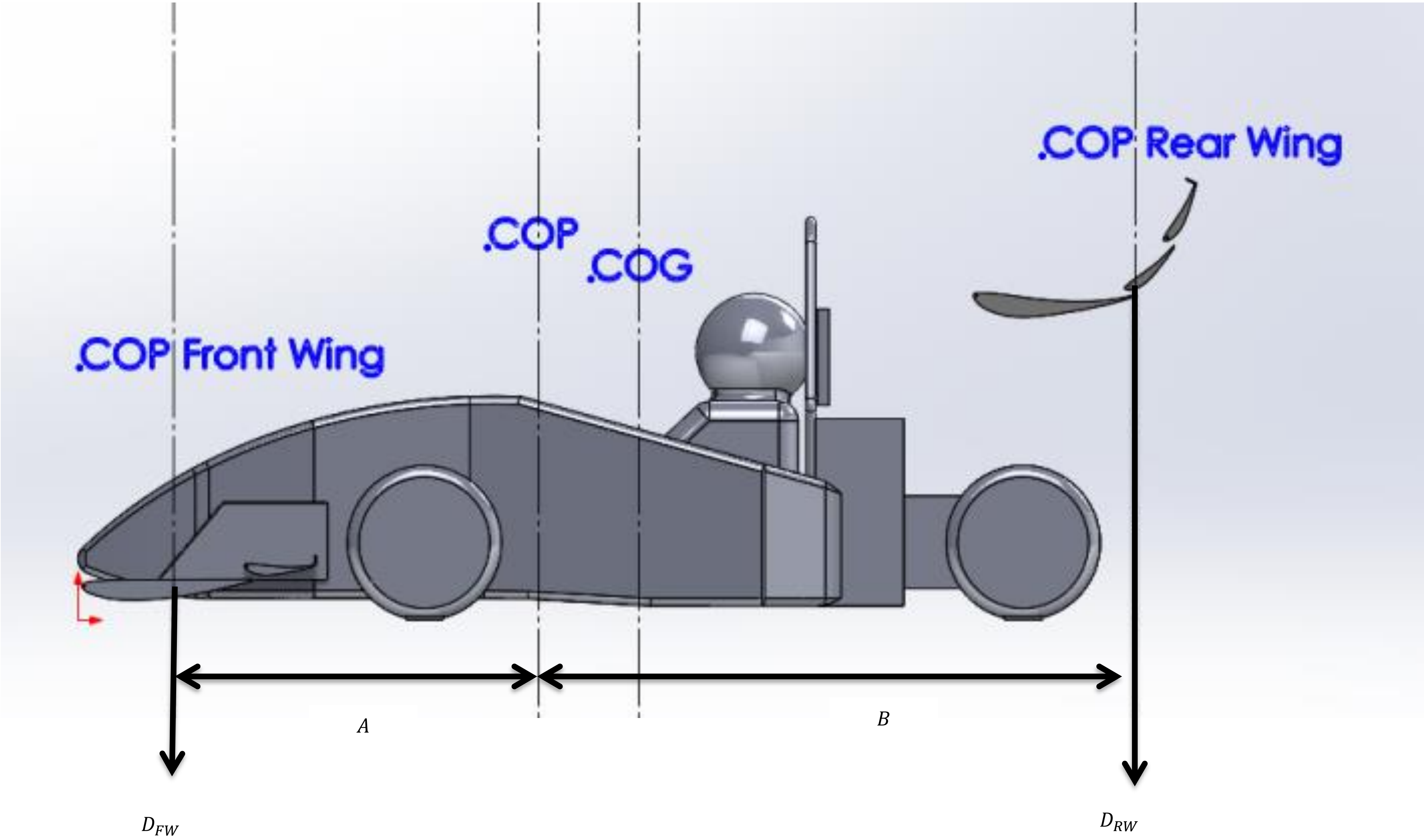

Appendix H: Chord Test

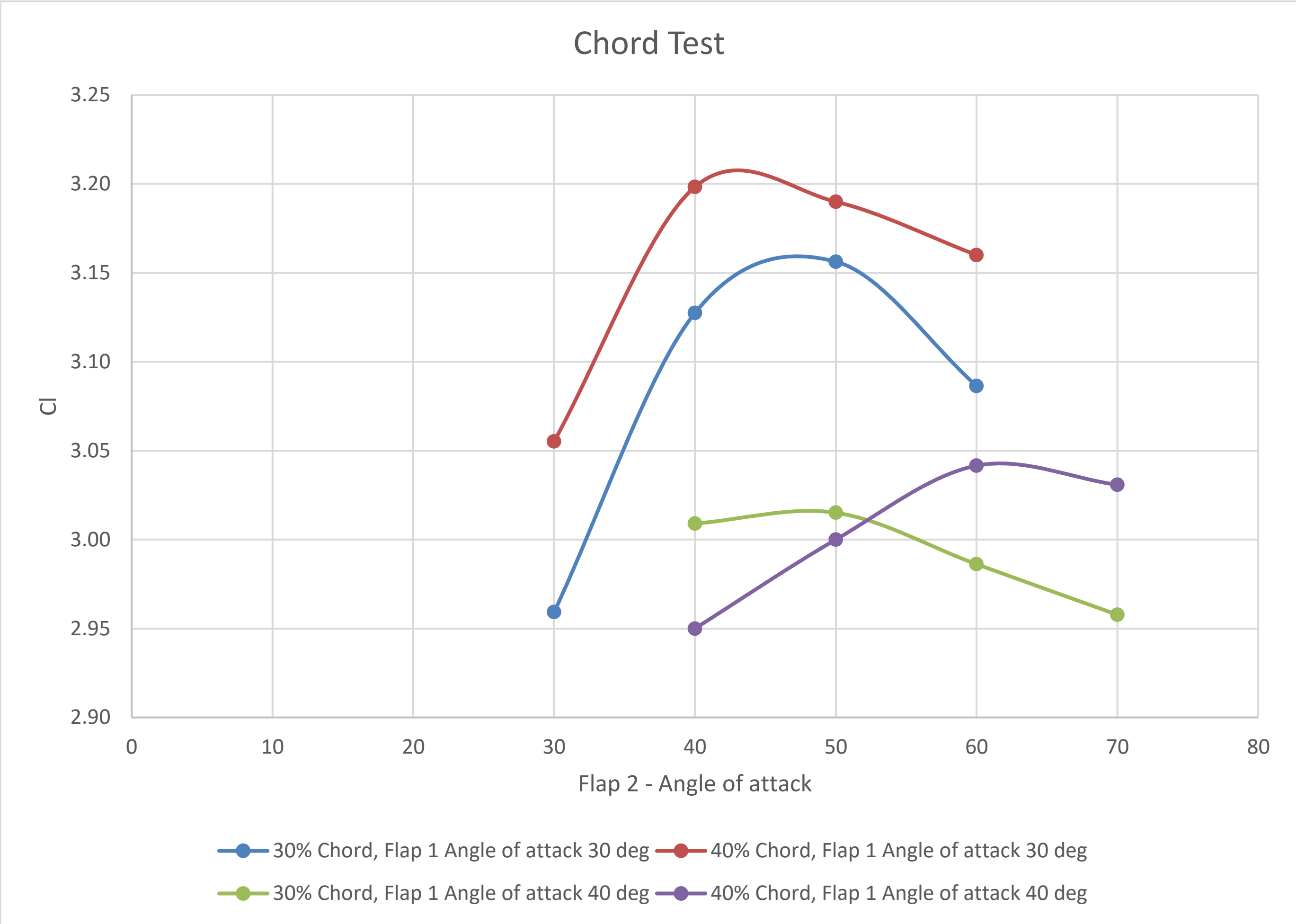

Appendix I: Mesh Study

Volume Mesh Study

Mesh Type	Number of Elements	Cl
200 mm volume sizing , 40 mm profile sizing, Inflation: 0.01 first layer height profile	2603426	2.2
100 mm volume sizing , 20 mm profile sizing, Inflation: 0.01 first layer height profile	3343279	2.2274
50 mm volume sizing , 10 mm profile sizing, Inflation: 0.01 first layer height profile	3861471	2.2303
25 mm volume sizing , 5 mm profile sizing, Inflation: 0.01 first layer height profile	7102072	2.23

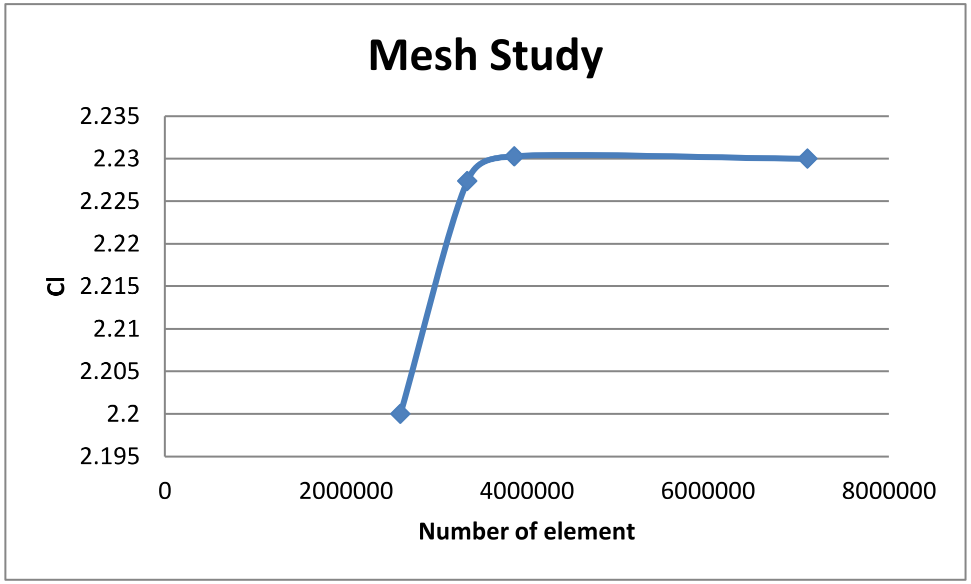

Inflation Mesh Study

Mesh Type	Number of Elements	Cl	Y+
100 mm volume sizing , 20 mm profile sizing, Inflation: 0.01 first layer height profile	3457630	2.20	1
100 mm volume sizing , 20 mm profile sizing, Inflation: 0.1 first layer height profile	2035981	2.17	10
100 mm volume sizing , 20 mm profile sizing, Inflation: 0.5 first layer height profile	1989266	2.22	30
100 mm volume sizing , 20 mm profile sizing, Inflation: 1 first layer height profile	1166944	2.22	60

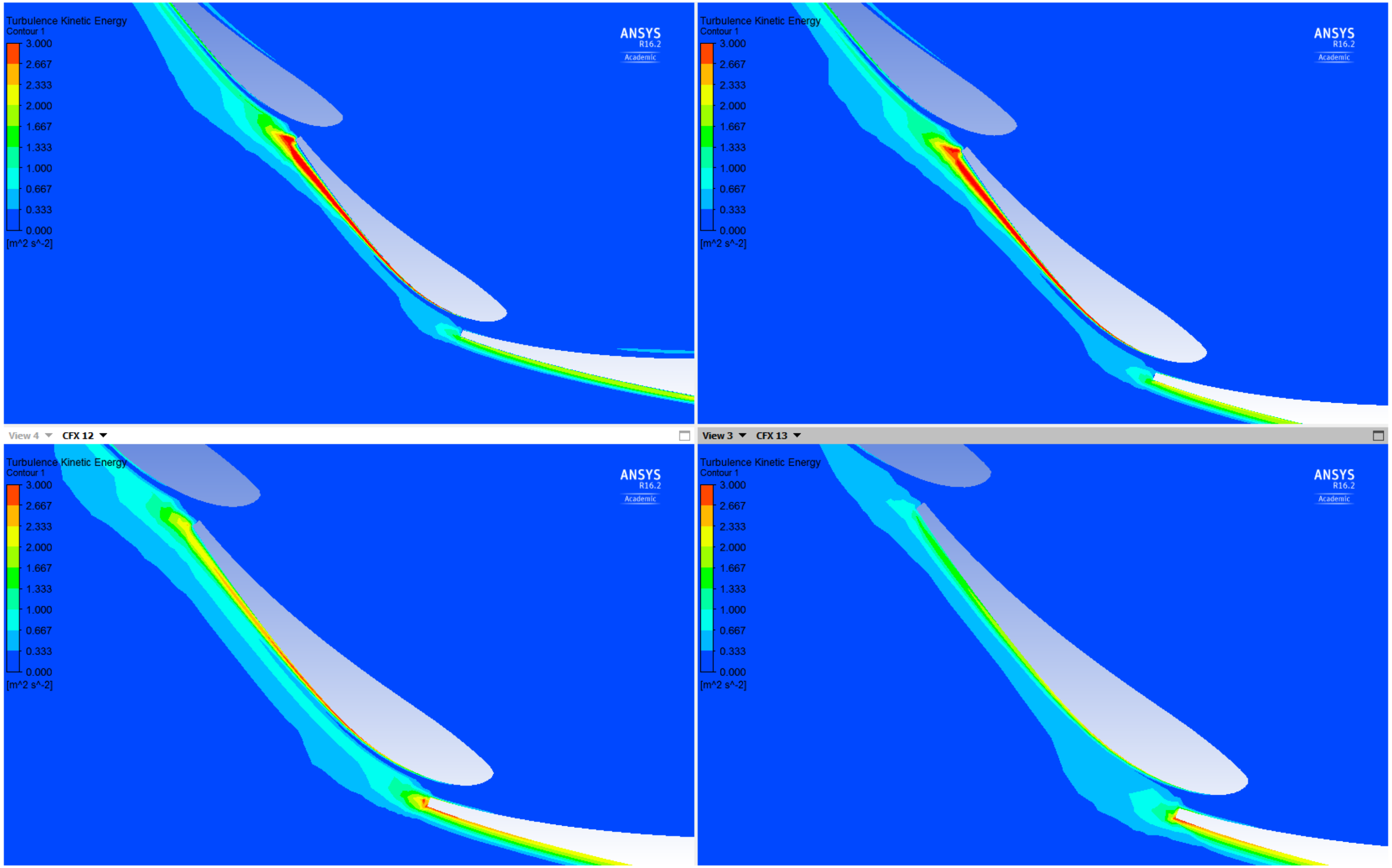

Y+1 top left, Y+10 top right, Y+ 30 bottom left and Y+ of 60 bottom right.

The difference between Cl is 1% but after a Y+ of 10 the flow structure changes of the second flap.

Appendix J: End Plate Length

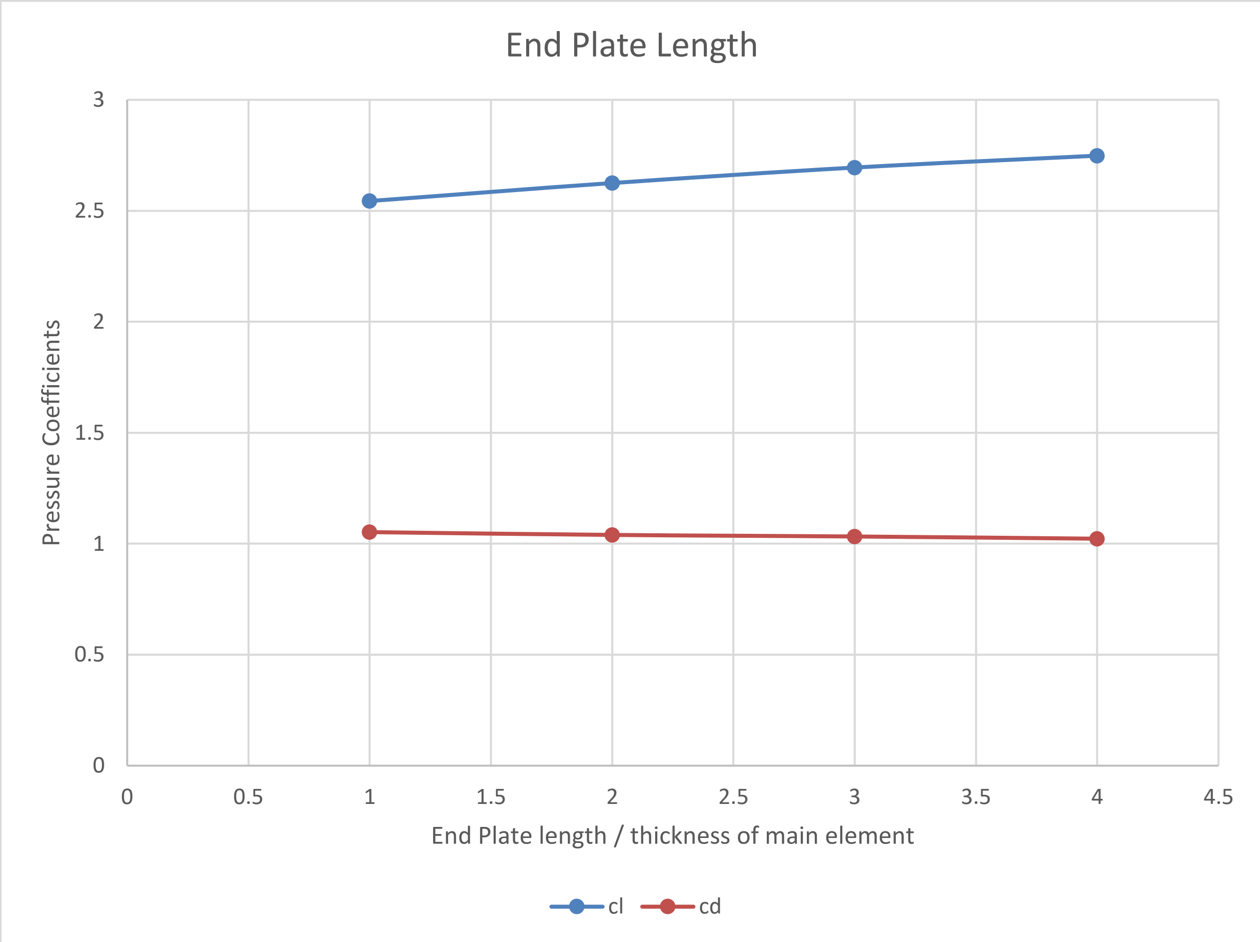

Appendix K: Front Wing Ground Clearance